

29 of population, and 50% of food production of China. Green water from western
30 provinces is the largest contributor to water resources, while green water from
31 southwestern and central provinces embodies the highest GDP, population, and food
32 production. Overall, the embodied socio-economic values of green water flow increase
33 from source to sink provinces, suggesting that green water from less developed
34 provinces effectively supports the higher socio-economic status of developed provinces.
35 The assessment emphasizes the substantial tele-connected socio-economic values of
36 green water flows and the need to incorporate them toward a more comprehensive and
37 effective water resources management.

38

39 **1 Introduction**

40 Terrestrial moisture recycling is a crucial process of the water cycle, whereby
41 water evaporates from land into the atmosphere, travels with prevailing winds, and
42 eventually falls back to the land as precipitation (van der Ent et al., 2010; Keys and
43 Wang-Erlandsson, 2018; Zemp et al., 2014). Terrestrial evapotranspiration (i.e., green
44 water) (Falkenmark and Rockström, 2006), which includes evaporation and
45 transpiration from land and vegetation, contributes to over half of the global
46 precipitation on land (van der Ent et al., 2010; Theeuwes et al., 2023; Tuinenburg et al.,
47 2020). Green water flows from upwind source regions to generate precipitation and
48 supply water resources for the social development of downwind sink regions through
49 moisture recycling (Schyns et al., 2019; Wang-Erlandsson et al., 2022). Analogous to
50 the upstream and downstream connection via blue water (referring to surface water and
51 groundwater flow within a watershed (Gleeson et al., 2020), the upwind source and
52 downwind sink regions are connected via green water flow within the evaporationshed
53 (i.e., downwind regions receiving precipitation from a specific location's evaporation)
54 (Ent and Savenije, 2013). Changes in both blue and green water flow directly impact
55 water resources availability, thereby influencing regional water security and human
56 societies (Keys et al., 2019).

57 The blue and green water flows provide a mechanism through which
58 upstream/upwind changes in ecohydrological and societal processes may affect the
59 downwind/downstream supply of water resources and, thus, ecological and societal
60 systems therein. Due to upstream water withdrawal and dams, global total blue water
61 flow into oceans and internal sinks decreased by 3.5% in 2002 compared to 1961–1990
62 (Döll et al., 2009). The decline in water availability exacerbated water stress in

63 downstream of transboundary river basins (Munia et al., 2016). Moreover, upstream
64 vegetation restoration, soil and water conservation practices reduced water yield
65 downstream, as already happened in the Yellow River (Wang et al., 2017; Zhou et al.,
66 2015b). Numerous studies have investigated the causal connection of blue water flow
67 from upstream and downstream regions, yet research into the connection of green water
68 flow from upwind and downwind regions and their impacts remains inadequate.

69 Unlike blue water flow primarily shaped by terrain with specific routes and
70 regulated by human activities (e.g., reservoir, transfer), green water flow is transported
71 by atmospheric air movement in a pervasive manner from evapotranspiration to
72 precipitation in downwind sink regions (Schyns et al., 2019). This establishes a spatial
73 linkage between source and sink regions for green water flow through the moisture
74 recycling process, similar to blue water flow through the surface hydrological process.
75 Therefore, evapotranspiration changes associated with land cover changes in source
76 regions are likely to impact not only downstream rivers via blue water flow but also
77 downwind precipitation via green water flow (Keys et al., 2012), with further
78 implications on socio-economic development (Wang-Erlandsson et al., 2018). For
79 example, vegetation greening reduced blue water but increased downwind water
80 availability globally through green water (Cui et al., 2022). Reduction in green water
81 in Amazon decreased downwind precipitation in the United States (Lawrence and
82 Vandecar, 2015), and reduction in green water source regions could decrease potential
83 crop yields in key global food-producing regions (Bagley et al., 2012).

84 Source regions supply water resources to support sink regions' socio-economic
85 development through both blue and green water flows. Existing research has
86 extensively assessed the socio-economic values of blue water, e.g., the population
87 dependency on runoff (Green et al., 2015; Viviroli et al., 2020), while seldom
88 considering the tele-connected effects of green water on socio-economy. In fact, green
89 water is also closely tied to human society because green water traveling from source
90 regions precipitates, recharges water resources, and ultimately sustains socio-economic
91 activities, livelihoods, and ecosystems in sink regions (Arag ão, 2012; Keys and Wang-
92 Erlandsson, 2018; O'Connor et al., 2021). These contributions should be quantified and
93 recognized as the value of green water to socio-economy, which expands the scope of
94 water management and water security maintenance (Keys et al., 2017; Rockström et al.,
95 2023). Emerging moisture tracking technologies offer feasible ways to quantify green
96 water flow across regions at large scale (Keys et al., 2019; Li et al., 2023; Theeuwens et

97 al., 2023) and pave the way for assessing the socio-economic values of green water.

98 The general spatial and seasonal patterns of moisture flows in China are
99 determined by regional atmospheric circulation systems, including prevailing westerly
100 winds (from the west toward the east) in most of China between 30° and 60° (Bridges
101 et al., 2023), the East Asian monsoon in eastern China, and India monsoon in
102 southwestern China. In summer, the East Asian and Indian monsoons supply moisture
103 for precipitation in eastern and southwestern China (Tian and Fan, 2013). In winter, the
104 East Asian monsoon drives northwesterly moisture transport across much of China and
105 generates precipitation (Wu and Wang, 2002). Recent studies analyzed the large-spatial
106 pattern of moisture recycling in China at the grid (Zhang et al., 2023), river basin (Wang
107 et al., 2023b), and ecological regions scales (Xie et al., 2024), or for specific regions
108 (Pranindita et al., 2022; Zhang et al., 2024). However, green water flows from different
109 regions are interlinked and become sources and sinks of each other. Such green water
110 transfer at a sub-national scale effectively forms an interconnected green water flow
111 network. It highlights the mutual dependency of green water and its socio-economic
112 contributions, especially for large countries like China. Few studies focus on green
113 water flows at the administrative district scale, which is important for water
114 management. Furthermore, the substantial regional disparities in socio-economic
115 development add complexity to understanding the socio-economic contributions of
116 green water among Chinese provinces. The western provinces with a weak economic
117 status and sparse populations are abundant in water resources (Ya-Feng et al., 2020). In
118 contrast, the economically developed and densely populated eastern provinces suffer
119 from water scarcity (Varis and Vakkilainen, 2001). Therefore, quantifying
120 interprovincial green water flows and evaluating the embedded socio-economic values
121 offer new perspectives for optimizing water resource utilization and mitigating the
122 imbalance in regional socio-economic development.

123 In this study, we used a high-quality moisture trajectory dataset from the UTrack
124 model to quantify and visualize the interprovincial network of green water flows within
125 China. Next, we combined socio-economic statistical data to evaluate socio-economic
126 values embodied in green water flow for economic production, population and food
127 production. Our study aims to reveal the transboundary green water flows within China
128 and their tele-connected effects on the socio-economy. This study incorporates green
129 water flow into water resources, extending water resources management beyond blue
130 water toward a more complete understanding of the water cycle and its socio-economic

131 implications, which is beneficial to assess and optimize regional water security.

132 **2 Data and Methods**

133 **2.1 Data**

134 This study used the moisture trajectory dataset generated by the Lagrangian
135 moisture tracking model “UTrack-atmospheric-moisture” driven by ERA5 reanalysis
136 data. The model is the state-of-the-art moisture tracking model, producing more
137 detailed evaporation footprints due to the high spatial resolution and reduced
138 unnecessary complexity (Tuinenburg and Staal, 2020). The dataset provides monthly
139 mean moisture flows at the global scale with a spatial resolution of 0.5° for 2008–2017,
140 expressed as the fractions of evaporation from a source grid allocated to precipitation
141 at a sink grid (Tuinenburg et al., 2020). It has been widely used in moisture recycling
142 research with various spatial scales, such as precipitation source of the grid (Staal et al.,
143 2023; Wei et al., 2024; Zhang et al., 2023) and basin scale (Wang et al., 2023b), and
144 moisture transport between nations (Rockström et al., 2023). The moisture trajectory
145 dataset was used in conjunction with the multi-year monthly mean ET of 2008–2017
146 from the ERA5 reanalysis dataset to estimate precipitation in a sink grid originating
147 from a source grid.

148 The socio-economic statistical data in 2008–2017 from the China Statistical
149 Yearbook were used to estimate the socio-economic values of green water in terms of
150 water resources volume, gross domestic product (GDP), population, and food
151 production for 31 provinces in mainland China, without Hong Kong, Macau, and
152 Taiwan due to the data limitation. GDP was adjusted to price in the year 2020 to
153 eliminate the effects of inflation.

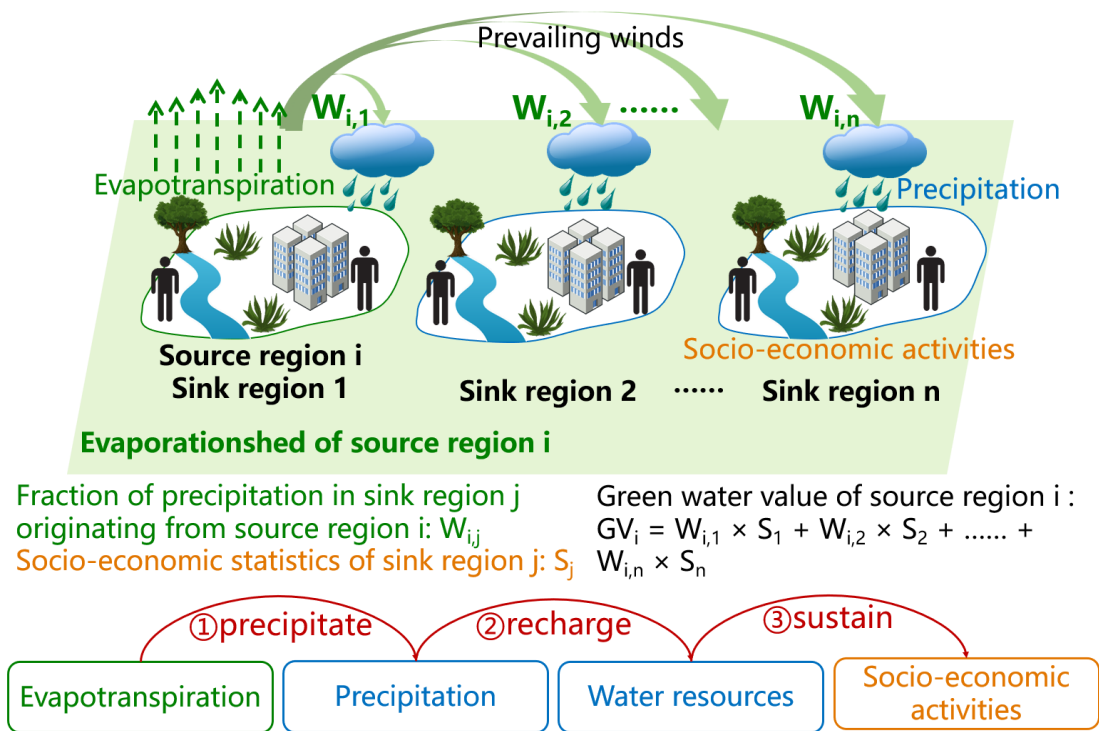
154 **2.2 Quantify green water flows in China**

155 We quantified interprovincial moisture flows and their precipitation contribution
156 following the workflow described in Fig. A1. At each sink grid, the ET to precipitation
157 fractions from the moisture trajectory datasets were multiplied by ERA5
158 evapotranspiration (ET) to obtain monthly precipitation contribution by moisture from
159 its source grids. Repeating the calculation for all grids within a sink province and
160 summing them up yielded the precipitation in the sink province contributed by each
161 source grid (Fig. A1 Step 1). Next, we employed zonal statistics to sum up precipitation
162 in the sink province contributed by grids of each source province, and the precipitation
163 contribution was converted to relative values, i.e., the fraction of precipitation in sink
164 province j originating from green water of a source province i (denoted as W_{ij}) rather

165 than absolute contribution to reduce the uncertainty in the latter (Fig. A1 Step 2). The
 166 fractions W_{ij} multiplied by the observed precipitation of the sink province restore the
 167 absolute precipitation contribution. This practice ensures that provincial precipitation
 168 is fully decomposed into different sources, avoiding the estimation bias of sink
 169 precipitation due to unclosed water balance by ET and precipitation data (De Petrillo et
 170 al., 2024). Finally, the interprovincial green water flows in China were derived after
 171 estimating each province individually.

172 The direction of green water flows can be represented by a vector starting from a
 173 source to sink province determined by their geometric centers and with its length
 174 denoting flow magnitude. Since green water flows have multiple destinations, each
 175 flow points to different sink provinces, and even outside of China. For each source
 176 province, all of their domestic green water flow vectors can be averaged to a composite
 177 to represent their net direction and magnitude, which are mainly determined by
 178 atmospheric wind conditions, source location and green water volume.

179 **2.3 Quantify socio-economic values embodied in green water**



180
 181 Figure 1. A conceptual diagram depicts the teleconnection of green water flows and their socio-
 182 economic contributions in a cascade manner. Evapotranspiration (green dotted arrows) from
 183 source region i flows downwind with prevailing winds (green thick arrows) and precipitates in
 184 sink region n , which recharges water sources and sustains socio-economic activities in sink
 185 regions.

186 Green water from upwind source provinces flows and precipitates downwind to

187 recharge water resources, and therefore sustains socio-economic activities in sink
 188 provinces, as depicted in Fig. 1. Consequently, precipitation, water resources, and
 189 socio-economic factors such as economic activities, human livelihood, and crop
 190 production in sink provinces rely on green water exported from source provinces.
 191 Changes in green water may affect water resource volume, and then impact economic
 192 activities, livelihood, and crop production through water supply. We chose water
 193 resources volume, economic output (measured by GDP), population, and food
 194 production as the four socio-economic indicators that are tightly related to water
 195 resources to evaluate the socio-economic contributions of green water.

196 If we assume all socio-economic activities in sink province j are sustained by
 197 precipitation which constitutes water resources and recharges groundwater, socio-
 198 economic statistics of sink province j can be partitioned to source provinces by their
 199 share of precipitation contribution (W_{ij}). Therefore, multiplying socio-economic
 200 statistics in sink province j (S_j) by W_{ij} yielded the socio-economic value of green water
 201 from source province i . The total socio-economic value of green water of source
 202 province i (GV_i) can be obtained by summing its contributions to all sink provinces (Fig.
 203 1), as equation (1):

$$204 \quad GV_i = \sum_{j=1}^n (W_{i,j} \times S_j), \quad (1)$$

205 where S_j is the average socio-economic value of 2008-2017 (i.e., water resources
 206 volume (km^3), GDP (in unit of CNY, 1 CNY = 0.14 USD), population (persons), and
 207 food production (ton)) at sink province j , n is the number of sink provinces.

208 Due to the different socio-economic development statuses, the same amount of
 209 green water may produce different socio-economic values between source and sink
 210 provinces. This means green water flow also involves changes in embodied socio-
 211 economic value from source to sink provinces. We used water productivity in the source
 212 province (WP_i) to calculate the socio-economic values of its exported green water in
 213 the counterfactual scenario when it was all consumed in the source province without
 214 interprovincial transfer (GV'_i) (Eq. 2). The results were compared with the actual green
 215 water's socio-economic values (Eq. 1) (namely socio-economic values of exported
 216 green water when it is consumed in sink provinces) as:

$$217 \quad GV'_i = \sum_{j=1}^n (W_{i,j} \times WU_j \times WP_i), \quad (2)$$

218 where WU_j is water use in sink province j , and WP_i is water productivity in source
 219 province i . (i.e., economic output, population, and food production per unit water use).

220 The changes in the socio-economic value of green water flow (ΔGV_i) from source

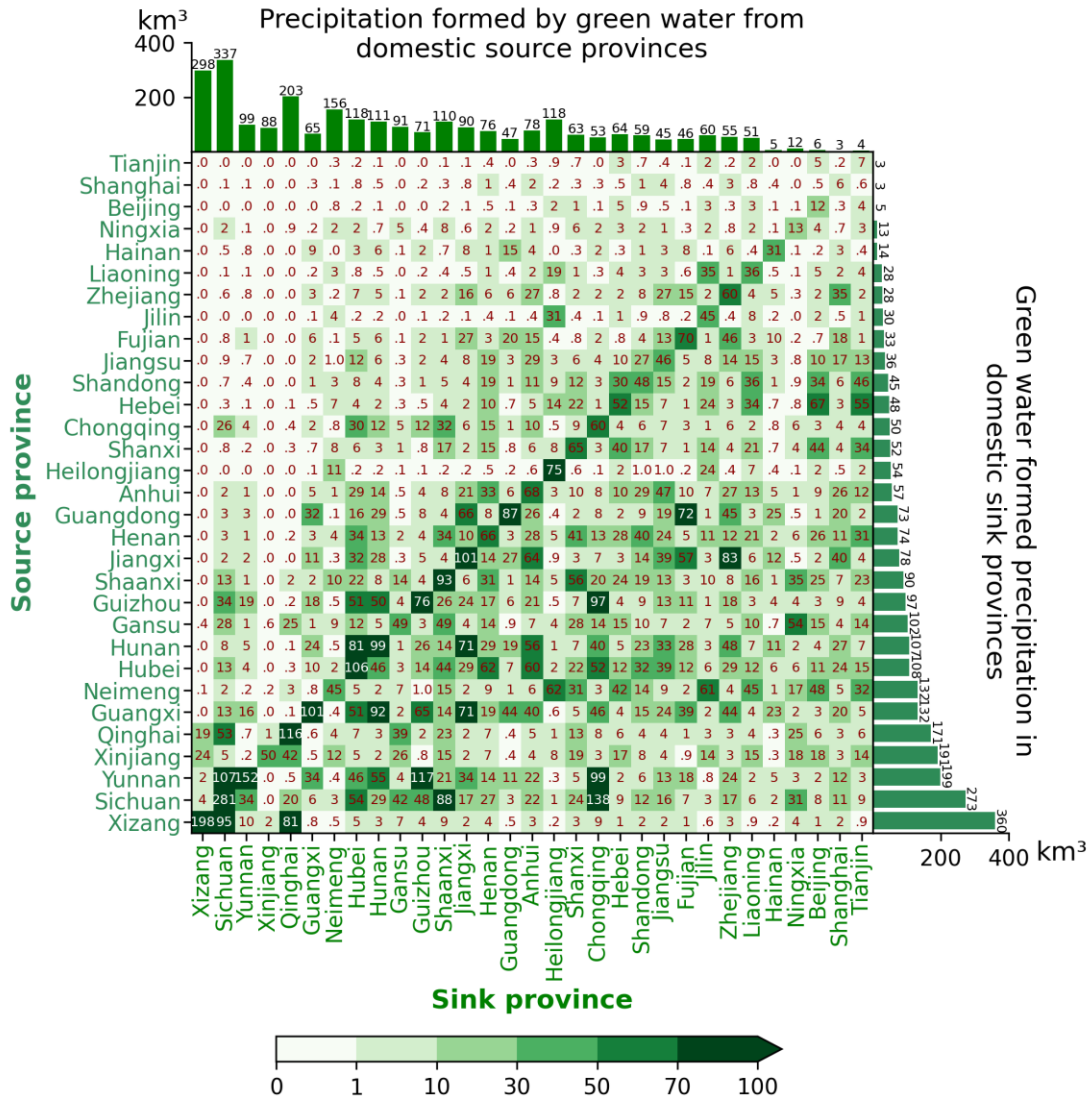
221 province i to its sink provinces can be estimated by Eq. 3.

222
$$\Delta GV_i = GV_i - GV'_i \tag{3}$$

223 $\sum_{i=1}^n \Delta GV_i$ is the net change in socio-economic values of all interprovincial
 224 green water flows in China.

225 **3 Results**

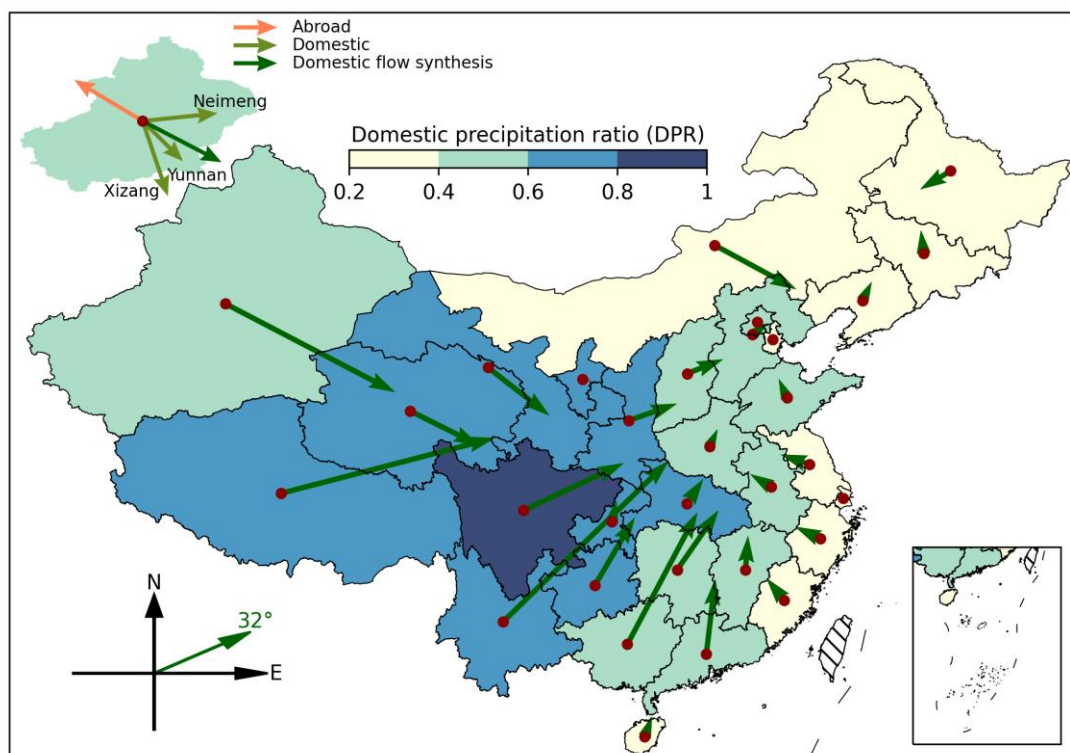
226 **3.1 The interprovincial green water flows in China and their directions**



227
 228 Figure 2. Interprovincial green water flows in China. The heat map denotes precipitation in sink
 229 province generated by green water from a source province (mm). The right bar shows domestic
 230 precipitation (km³) formed by green water from each source province. The top bar shows
 231 precipitation in each sink province formed by green water from domestic source provinces (km³).
 232 Green water exported from a source province forms precipitation in different sink
 233 provinces in China, and precipitation in a sink province originates from green water in

234 different source provinces. Therefore, different provinces in China, acting either as
 235 sources or sinks, are interconnected through moisture recycling and established an
 236 interprovincial network (Fig. 2).

237 A large fraction of green water exported from each source province is retained
 238 locally to generate precipitation (diagonal cells in Fig. 2). The precipitation recycling
 239 ratio (PRR), the ratio of precipitation generated by local green water to total
 240 precipitation, reflects how much green water of each source province contributes to its
 241 own precipitation (Fig. A2c). Xizang has the highest PRR of 0.345, followed by
 242 Qinghai (0.341) and Sichuan (0.297). Besides local recycling, green water
 243 predominantly flows and generates more precipitation in neighboring provinces and
 244 less in distant provinces. For example, green water from Sichuan forms high
 245 precipitation in neighboring provinces such as Chongqing (138 mm), far surpassing
 246 other distant sink provinces (< 88 mm).



247
 248 Figure 3. Direction of green water flows from each source province in China. Green arrows
 249 indicate the average direction of domestic green water flows, denoted as a vector starting from a
 250 source (the geometric center in red points) to sink provinces and with its length representing the
 251 amount of precipitation formed by green water. The face colors on the map represent fractions of
 252 green water formed precipitation within China of each source province (DPR). The upper left
 253 corner is a schematic diagram for green water flows from Xinjiang. The lower left corner is the
 254 composite flow direction of interprovincial green water of all provinces.

255 The direction of interprovincial green water flow can be visualized as a composite

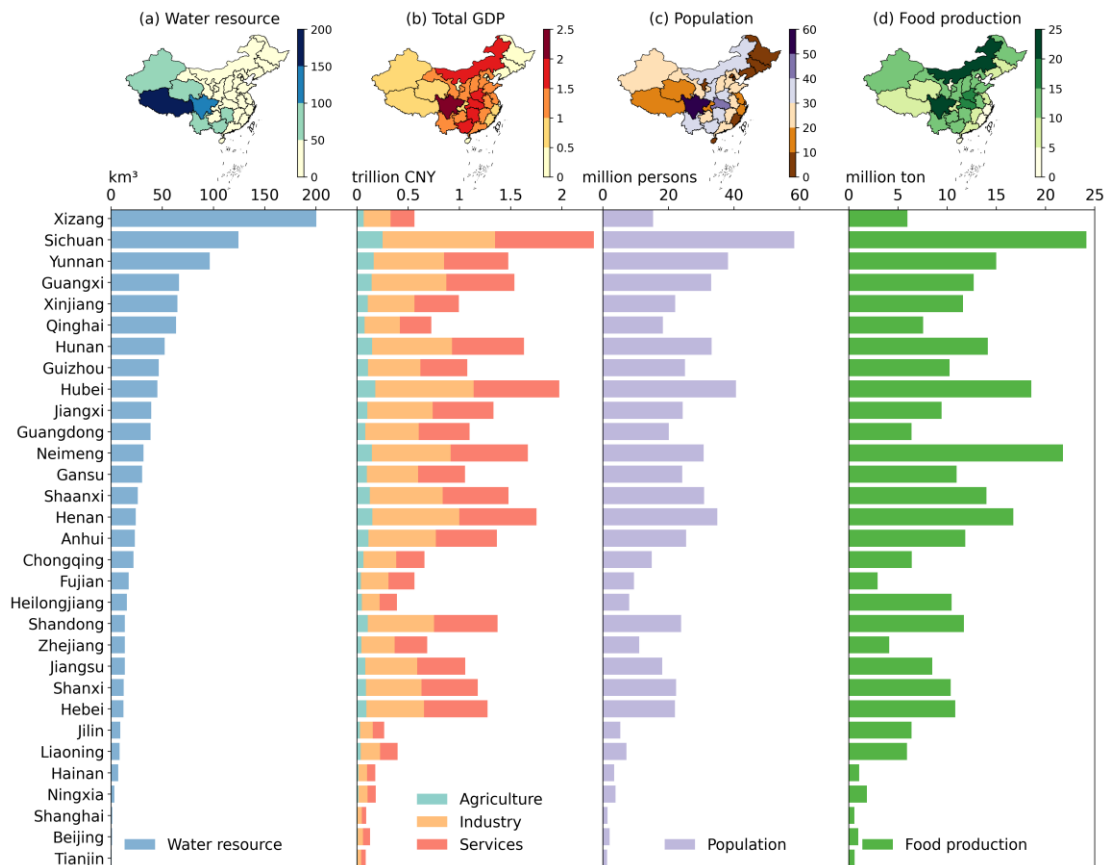
256 direction averaging all domestic green water flows from each source province, which
257 are mainly determined by atmospheric wind conditions, source location, and green
258 water volume (Fig. 3). Overall, the average direction of all interprovincial green water
259 flows is at 32° northeastward (32° north off the east direction), suggesting green water
260 within China is transported to the north and east directions owing to combined effects
261 of monsoons and westerly.

262 Green water exported by source provinces contributes to precipitation both within
263 and outside China. We defined the domestic precipitation ratio (DPR) as the ratio of
264 green water that formed precipitation in China to each province's total green water
265 export to represent their relative importance to China's precipitation (Fig. A2a). Green
266 water from provinces in western and central China mainly flows eastward under the
267 influence of prevailing westerlies, which extend their evaporationsheds eastward to
268 cover a large territory of China and generate more precipitation within China (Fig. 3).
269 For instance, green water from Xizang, the largest exporter in China, produces the
270 largest domestic precipitation (360 km³) (right bar on Fig 2) with a high DPR of 0.74,
271 contributing to precipitation in other 30 provinces with varying extents (0.2 to 95 mm).
272 Similarly, the green water from southern provinces is affected by the Indian Ocean
273 Monsoon (southwest monsoon), which drives green water flowing northeastward. With
274 a substantial volume of green water, these southern provinces contribute significantly
275 to domestic precipitation. In contrast, green water from eastern coastal or northwest
276 border provinces goes to the northwest primarily attributed to the East Asian Monsoon
277 (southeast monsoon) (Cai et al., 2010). As a result, most evaporationsheds laid outside
278 China generate less domestic precipitation but more outside the country, resulting in a
279 lower DPR, such as Fujian (DPR 0.31) and Heilongjiang (DPR 0.23). The northern
280 provinces are influenced by westerly winds and winter monsoon from Siberia (Sun et
281 al., 2012), causing predominantly southeastward flow of green water. However,
282 evaporationsheds of these provinces mainly cover the Pacific Ocean, resulting in a
283 relatively low DPR despite their substantial volume of exported green water. While
284 some inland provinces have a high DPR because their evaporationsheds overlap with
285 mainland China, the low green water volume (Fig. A4) limits their domestic
286 precipitation contribution (e.g., Gansu and Ningxia with DPR of 0.72 and 0.66,
287 respectively).

288 Furthermore, precipitation in sink provinces originates from both domestic and
289 foreign green water sources. Sichuan (337 km³), Xizang (298 km³), and Qinghai (203

290 km³) are the top 3 provinces importing the largest volume of green water from domestic
 291 sources due to the large ET from themselves and neighboring provinces (top bar of Fig
 292 2). To quantify the relative importance of domestic sources, we defined the domestic
 293 source ratio (DSR) in each province as the sum of precipitation contribution from
 294 domestic sources divided by total precipitation (Fig. A2 (b)). DSR is related to each
 295 province's precipitationshed (i.e., upwind region contributing evaporation to a specific
 296 location's precipitation) (Keys et al., 2014) and the included domestic green water
 297 exporters. The highest DSR found in Qinghai (0.86) and Ningxia (0.82) is because their
 298 precipitationsheds include large domestic green water exporters like Xinjiang and
 299 Xizang, which supply considerable green water traveling eastward. Conversely, Hainan
 300 (0.07) and Guangdong (0.14) in coastal areas have lower DSR because their
 301 precipitationsheds are primarily located in oceans and other countries due to the
 302 influence of the summer monsoon (Cai et al., 2010).

303 3.2 Socio-economic values embodied in interprovincial green water 304 flows



305
 306 Figure 4. The embodied socio-economic values of green water flow from source provinces for
 307 water resources, GDP, population, and food production (average value of 2008-2017) of sink
 308 provinces in China.

309 Source provinces export green water and create precipitation to sink provinces
310 through moisture recycling process, recharging water resources and sustaining the
311 socio-economic development of downwind sink provinces (Fig. 4). The reliance of
312 socio-economic activities in sink provinces on green water supply from source
313 provinces implies that the green water and socio-economy are intertwined through the
314 interprovincial green water flow network, indicating a teleconnection between source
315 and sink provinces.

316 Our assessment of contribution of green water to water resources indicates that
317 green water from western provinces recharges the highest volume of water resources.
318 Xizang (200 km³), Sichuan (124 km³), and Yunnan (96 km³) are the top 3 contributors
319 of water resources, whose green water export makes up 46%, 51%, and 52% of their
320 own total water resources, respectively (Table. A1). These regions also correspond to
321 the top contributors to domestic precipitation, owing to the close linkage between
322 precipitation and water resources. Although southern and eastern provinces are rich in
323 water resources due to the wet climate, most of their green water contributes to water
324 resources outside of China or to the ocean since they are situated downwind of
325 prevailing westerlies and proximate to the coast (e.g., Guangdong). In total, green water
326 exported from 31 provinces contributes 43% and 40% of precipitation and water
327 resources in China (Table. A1).

328 The GDP, population, and food production embodied in green water export from
329 source provinces are shown in Fig 5b-d, which reflects how much the socio-economy
330 of downwind sink provinces is supported by green water of source provinces. Overall,
331 the contribution of green water to selected socio-economic statistics shows similar
332 rankings because food production and agriculture GDP ($R = 0.79$), population and total
333 GDP ($R = 0.85$) are spatially correlated (Fig. A6).

334 Sectoral GDP embodied in green water from source provinces is highly related to
335 the industrial structure in sink provinces. The embodied industry and service sector
336 GDP values across provinces are relatively comparable, whereas embodied agricultural
337 GDP values are lower due to the small percentage of agricultural output to total GDP
338 (Fig. A3).

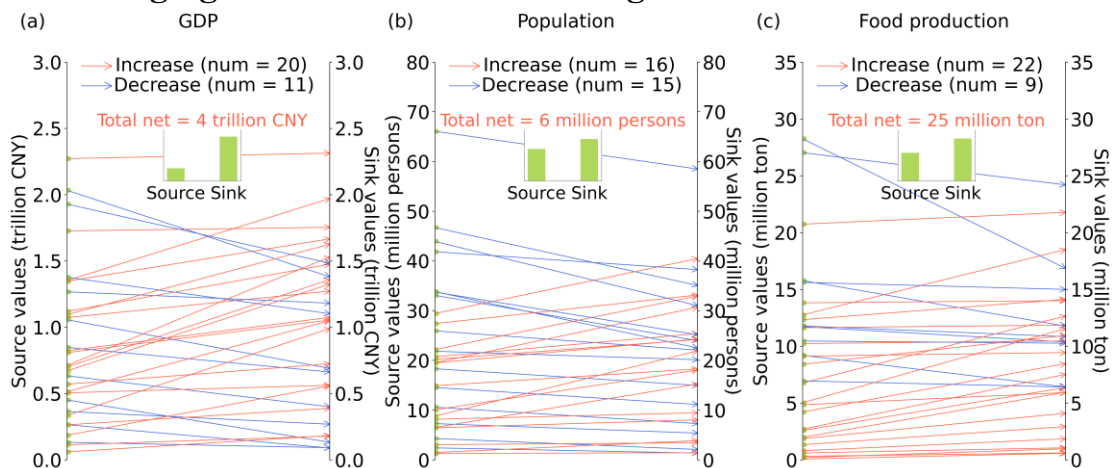
339 Green water from southwest and central provinces (e.g., Sichuan, Hubei, Henan)
340 embodies the most GDP, population, and food production because of the large
341 economic volume of these provinces and neighboring regions, as well as the high DPR.
342 Specifically, green water from Sichuan supports the highest GDP (2.31 trillion CNY),

343 population (58 million persons), and food production (24 million tons) (Table. A2)
 344 because Sichuan has a high GDP, population, and food production (Fig. A3). Moreover,
 345 green water from Sichuan contributes significantly to its own precipitation (30%), and
 346 87% of its green water generates domestic precipitation. These factors together make
 347 green water in provinces like Sichuan embody the highest socio-economic values.

348 Provinces that export large volumes of green water and have high DPR do not
 349 necessarily embody more socio-economic values if sink provinces that import their
 350 green water are less developed. Xizang is the highest green water exporter and the
 351 largest contributor of water resources (200 km³) but ranks low in embodied GDP (0.56
 352 trillion CNY, 23rd), population (15 million, 20th), and food production (5.97 million tons,
 353 23rd) because the primary importer of its green water, such as Xizang and Qinghai, have
 354 low rankings in GDP (31st, 30th), population (31st and 30th), and food production (30th
 355 and 29th).

356 Green water from highly developed provinces (e.g., southeastern China) may not
 357 necessarily embody high socio-economic value if they have low DPR. For example,
 358 Guangdong ranks 1st in GDP and population and 17th in food production but only has a
 359 small fraction of green water contributing to domestic precipitation (DPR 0.4). The
 360 limited domestic precipitation contribution results in low rankings of embodied socio-
 361 economic values (14th for GDP, 17th for population, and 21st for food production) for
 362 Guangdong.

363 3.3 Changing socio-economic values of green water flows



364
 365 Figure 5. Changes in socio-economic values embodied in green water flow from source to sink
 366 provinces for GDP (a), population (b), and food production (c). Thin arrows of different colors
 367 represent the socio-economic value increase (in red) or decrease (in blue) from source to sink
 368 provinces. Green bars represent the sum socio-economic value in China's 31 provinces.

369 The substantial socio-economic values embodied in interprovincial green water

370 flows highlight the teleconnection of green water from source provinces and the socio-
371 economy in sink provinces, including economy, population, and food production. Due
372 to different socio-economic statuses, the same amount of consumed water resources,
373 which are recharged by green water, would sustain different socio-economic values
374 between source and sink provinces. Therefore, the socio-economic values embodied in
375 green water flow would change when traveling from source to sink provinces. As shown
376 in Fig. 5, the socio-economic values embodied in green water flow increase from source
377 to sink provinces by 4 trillion CNY for GDP, 6 million for population, and 25 million
378 tons for food production, respectively. The increase in the embodied GDP, population,
379 and food production is observed in 20, 16, and 22 source provinces among a total of 31.
380 This indicates that green water tends to flow from less to more developed provinces,
381 sustaining more economic production, population, and food production per unit of
382 green water. The largest economic output value increases are in Guangxi (+0.83 trillion
383 CNY, 54%). Xinjiang has the most added value in population (+13 million persons,
384 59%) and food production (+7 million tons, 60%) because their green water flows to
385 more developed provinces (Fig. A5). In contrast, decreased socio-economic values of
386 green water flow are also observed. Shandong, Shaanxi, and Henan have the largest
387 depreciation in green water values for GDP (-0.66 trillion CNY, 48%), population (-13
388 million persons, 42%), and food production (-12 million tons, 72%) (Fig. A5) because
389 their green water flows to provinces with lower socio-economic values.

390 The changing socio-economic values of green water flow reflect the regional
391 disparity in socio-economic statuses between source and sink provinces. The exported
392 green water for more than half of the source provinces in China (> 15) has increased
393 socio-economic values when reaching sink provinces. This shows that green water from
394 less developed provinces effectively supports the higher socio-economic status of
395 developed provinces through the interprovincial flow network. Therefore, these
396 provinces are vitally important green water providers to developed areas. This
397 teleconnection of green water and socio-economy substantiates that changing land use
398 in the source provinces that affect evapotranspiration is likely to influence water
399 resources availability and socio-economic development in the sink provinces (Dias et
400 al., 2015; Weng et al., 2018). Hence, it is imperative to account for “invisible” green
401 water flow and its cascade effect in large-scale water resources management.

402 **4 Discussion**

403 This study quantified the interprovincial green water flows in China using the

404 moisture recycling framework and a moisture tracking model. The green water flow is
405 established by transporting evaporated moisture by atmospheric winds from a source
406 province to precipitate in a sink province. The transferred green water exchanges among
407 multiple provinces and creates an interprovincial flow network. The location of the
408 source province and its flow direction largely determine to what extent green water
409 formed precipitation retains within China. In our estimation, roughly 43% of green
410 water forms precipitation in China, similar to 44% of PRR identified by Rockström et
411 al. (2023). The average direction of all interprovincial green water flows in China is
412 from southwest to northeast, consistent with findings by Xie et al. (2024).

413 Green water flow can fill the gap in land-atmosphere feedback in the traditional
414 water resources management framework (Keys et al., 2017). Typically, water resources
415 management only considers blue water changes while neglecting green water flow,
416 even though the latter may compensate for the former (Hoek van Dijke et al., 2022).
417 Human activities such as irrigation (Su et al., 2021), afforestation (Li et al., 2018), and
418 reservoir construction (Biemans et al., 2011; Veldkamp et al., 2017) in upstream regions
419 may markedly change blue water accessibility in downstream regions. Meanwhile, the
420 resulting changes of ET in upstream regions (McDermid et al., 2023; Qin, 2021; Shao
421 et al., 2019) might offset the decline of water resources in downstream by moisture
422 recycling. Similarly, increased vegetation coverage intercepts more rainfall, reducing
423 runoff and consequently diminishing water resources availability (Sun et al., 2006;
424 Zhou et al., 2015a), but the rise of ET may compensate for local and downwind water
425 availability through increased green water flows (Wang et al., 2023a; Zhang et al.,
426 2021). Therefore, green water is an essential path of climatic and hydrological
427 interaction among different regions, providing a new angle for integrated regional
428 resources management (Keys et al., 2018; te Wierik et al., 2021). A comprehensive
429 impact assessment of regional water security and optimization would benefit from
430 combining both blue and green water flows (Schyns et al., 2019) by which
431 upstream/upwind regions affect regional water resource availability (Creed et al., 2019).

432 With the recognition of the tele-connected effects of green water flows,
433 maintaining regional water security requires both rational utilization of local water
434 resources and appropriate land management in the upwind source regions. However,
435 similar to blue water, water resource management across administrative boundaries has
436 always been challenging due to conflicting interests among different regions
437 (Rockström et al., 2023). The diverse strategies developed to enhance regional

438 coordination of blue water management serve as a reference for green water
439 management, such as the inter-basin water transfer or downstream beneficiaries paying
440 upstream providers for clean water services (Farley and Costanza, 2010; Pissarra et al.,
441 2021; Sheng and Webber, 2021). However, unlike blue water resources with well-
442 established accounting and valuation methods, green water monitoring and valuation
443 are challenging. Green water from a specific region flows to multiple regions, and the
444 received green water can subsequently reevaporate and flow to other regions (Zemp et
445 al., 2014). This interconnected network and cascade complicate the quantification of
446 how much green water from a source region contributes to human activities in sink
447 regions. More importantly, it is difficult to measure green water flow through
448 observations as those measurements made by hydrologic stations for blue water (Hu et
449 al., 2023; Sheng and Webber, 2021). This study utilized a dataset from a moisture
450 tracking model to construct an interprovincial green water flow within China, which
451 offers valuable insights for understanding the quantity of green water flow.

452 Due to the complex dynamics of the green water flow and limitations of the
453 moisture tracking model, there are still major uncertainties in data and methods of this
454 study. First, ET and precipitation datasets driving the UTrack model affect the tracked
455 trajectories and magnitude of moisture flow. The resulting moisture trajectory is
456 expressed as the fraction of ET to precipitation, and the exact amount of moisture is
457 restored by the ET and precipitation datasets chosen by users. Different ET and
458 precipitation datasets could lead to different precipitation contributions and PRR (Li et
459 al., 2023). We used the ERA5 dataset to keep consistent with the original UTrack model.
460 It is noted that the non-closure of the moisture balance from ERA5 (De Petrillo et al.,
461 2024) and simplifications and assumptions introduced in the moisture tracking model
462 also add uncertainty in the moisture tracking (Tuinenburg and Staal, 2020). Moreover,
463 the resulting moisture trajectory data only represent the climatologically average
464 moisture trajectories and ET (Li et al., 2023), neglecting the interannual variability in
465 moisture flow trajectory, e.g., those induced by the influence of extreme weather events
466 or ENSO (Zhao and Zhou, 2021). The interannual variations in green water flow may
467 affect DPR and DSR in some provinces. Human adaptation tends to buffer the impacts
468 of interannual variations on the socio-economy through water resource management
469 such as reservoirs, dams, and other infrastructure. Accounting for interannual variations
470 in green water flows and their socio-economic contribution is worth further
471 investigation. Secondly, the socio-economic value assessment of green water in this

472 study only considers green water flows within China, excluding flows moving abroad
473 and to the ocean that may embody socio-economic value beyond the territory of
474 mainland China. We mainly attribute socio-economic values to green water and
475 generated precipitation because precipitation is the ultimate water source for recharging
476 surface and groundwater of a region. Strictly speaking, such attribution needs to be
477 more precise because socio-economy also utilizes streamflow from upstream areas,
478 which deserve separate attention.

479 Moreover, the interactions between blue and green water increase the complexity
480 to evaluating green water's socio-economic contribution. For example, the blue water
481 extracted by irrigation increases ET in the source region, providing more moisture for
482 downwind regions (Yang et al., 2019). Simultaneously, most of the blue water for local
483 irrigation comes from the green water of upwind regions (McDermid et al., 2023). In
484 addition, not all water resources replenished by green water-induced precipitation are
485 accessible for human activities since part of them is used by the natural ecosystem
486 (Keys et al., 2019). Therefore, it is necessary to distinguish water sources and
487 consumption to account green water values more accurately. Despite the selected socio-
488 economic indicators closely linked to water resources, green water flows' socio-
489 economic contribution can manifest in other aspects such as livestock production and
490 irrigated agriculture. In future studies, the dynamic linkage between green water, water
491 resources and economic development can be assessed annually by using a long-term
492 moisture tracking dataset with a separation of water sources consumed by socio-
493 economy (surface and groundwater). Nevertheless, our assessment serves as a useful
494 first step to demonstrate the importance of the tele-connected green water flow in
495 addition to blue water. Our attempts to quantify the socio-economy embodied in green
496 water flow fill the gap in green water value assessment and provide a methodological
497 reference for green water management.

498 **5 Conclusion**

499 This study quantified the interprovincial green water flows in China and its tele-
500 connected effects on the socio-economy. The green water exchanges among different
501 regions effectively form a complex flow network and embody socio-economic values.
502 The interprovincial green water in China flows primarily from west to east and to a
503 lesser extent from south to north, influenced by the co-control of westerlies and
504 monsoons. Western provinces have significant contributions to precipitation and water
505 resources in China, while southwestern and central provinces have the most socio-

506 economic values regarding GDP, population, and food production. Green water flowing
507 from less developed regions supports substantial socio-economic values in more
508 affluent regions due to disparity in socio-economic development between source and
509 sink regions. Given the embodied socio-economic benefits of green water, regional
510 water resources management should consider water flow beyond blue water to integrate
511 green water for a more comprehensive and effective management of resources and
512 security. Our study provides a reference for understanding the “invisible” green water
513 flow and its tele-connected benefits.

514 **Data and code availability**

515 The moisture trajectory dataset is available at
516 <https://doi.pangaea.de/10.1594/PANGAEA.912710> (Tuinenburg et al., 2020). The
517 evapotranspiration data from ERA5 reanalysis dataset is available at
518 <https://cds.climate.copernicus.eu/#!/search?text=ERA5>. The socio-economic statistics
519 data is available from China Statistical Yearbook (<https://data.stats.gov.cn/index.htm>).

520 The Python codes and data used in this study are available at GitHub
521 (<https://github.com/sangshan-ss/GW-China>).

522 **Author contributions**

523 YL and SS conceived the study and performed data analysis. SS and YL wrote the
524 manuscript with contributions from CCH, SSZ and HQL.

525 **Competing interests**

526 We declare no conflict of interest of this work.

527 **Financial support**

528 This research was funded by the National Natural Science Foundation of China
529 (42041007), the Second Tibetan Plateau Scientific Expedition and Research Program
530 (2019QZKK0405) and the Fundamental Research Funds for the Central Universities.

531 **References**

532 Aragão, L. E. O. C.: The rainforest’s water pump, *Nature*, 489, 217–218,
533 <https://doi.org/10.1038/nature11485>, 2012.

534 Bagley, J. E., Desai, A. R., Dirmeyer, P. A., and Foley, J. A.: Effects of land cover
535 change on moisture availability and potential crop yield in the world’s breadbaskets,
536 *Environ. Res. Lett.*, 7, 014009, <https://doi.org/10.1088/1748-9326/7/1/014009>, 2012.

537 Biemans, H., Haddeland, I., Kabat, P., Ludwig, F., Hutjes, R. W. A., Heinke, J.,
538 Bloh, W. von, and Gerten, D.: Impact of reservoirs on river discharge and irrigation
539 water supply during the 20th century, *Water Resources Research*, 47,
540 <https://doi.org/10.1029/2009WR008929>, 2011.

541 Bridges, J. D., Tarduno, J. A., Cottrell, R. D., and Herbert, T. D.: Rapid
542 strengthening of westerlies accompanied intensification of Northern Hemisphere

- 543 glaciation, *Nat Commun*, 14, 3905, <https://doi.org/10.1038/s41467-023-39557-4>, 2023.
- 544 Cai, Y., Tan, L., Cheng, H., An, Z., Edwards, R. L., Kelly, M. J., Kong, X., and
545 Wang, X.: The variation of summer monsoon precipitation in central China since the
546 last deglaciation, *Earth and Planetary Science Letters*, 291, 21–31,
547 <https://doi.org/10.1016/j.epsl.2009.12.039>, 2010.
- 548 Creed, I. F., Jones, J. A., Archer, E., Claassen, M., Ellison, D., McNulty, S. G., van
549 Noordwijk, M., Vira, B., Wei, X., Bishop, K., Blanco, J. A., Gush, M., Gyawali, D.,
550 Jobbágy, E., Lara, A., Little, C., Martin-Ortega, J., Mukherji, A., Murdiyarso, D., Pol,
551 P. O., Sullivan, C. A., and Xu, J.: Managing Forests for Both Downstream and
552 Downwind Water, *Front. For. Glob. Change*, 2,
553 <https://doi.org/10.3389/ffgc.2019.00064>, 2019.
- 554 Cui, J., Lian, X., Huntingford, C., Gimeno, L., Wang, T., Ding, J., He, M., Xu, H.,
555 Chen, A., Gentine, P., and Piao, S.: Global water availability boosted by vegetation-
556 driven changes in atmospheric moisture transport, *Nat. Geosci.*, 15, 982–988,
557 <https://doi.org/10.1038/s41561-022-01061-7>, 2022.
- 558 De Petrillo, E., Fahrländer, S., Tuninetti, M., Andersen, L. S., Monaco, L., Ridolfi,
559 L., and Laio, F.: Reconciling tracked atmospheric water flows to close the global
560 freshwater cycle, <https://doi.org/10.21203/rs.3.rs-4177311/v1>, 30 April 2024.
- 561 Dias, L. C. P., Macedo, M. N., Costa, M. H., Coe, M. T., and Neill, C.: Effects of
562 land cover change on evapotranspiration and streamflow of small catchments in the
563 Upper Xingu River Basin, Central Brazil, *Journal of Hydrology: Regional Studies*, 4,
564 108–122, <https://doi.org/10.1016/j.ejrh.2015.05.010>, 2015.
- 565 Döll, P., Fiedler, K., and Zhang, J.: Global-scale analysis of river flow alterations
566 due to water withdrawals and reservoirs, *Hydrology and Earth System Sciences*, 13,
567 2413–2432, <https://doi.org/10.5194/hess-13-2413-2009>, 2009.
- 568 Ent, R. J. van der and Savenije, H. H. G.: Oceanic sources of continental
569 precipitation and the correlation with sea surface temperature, *Water Resources*
570 *Research*, 49, 3993–4004, <https://doi.org/10.1002/wrcr.20296>, 2013.
- 571 van der Ent, R. J., Savenije, H. H. G., Schaeffli, B., and Steele-Dunne, S. C.: Origin
572 and fate of atmospheric moisture over continents, *Water Resources Research*, 46,
573 <https://doi.org/10.1029/2010WR009127>, 2010.
- 574 Falkenmark, M. and Rockström, J.: The New Blue and Green Water Paradigm:
575 Breaking New Ground for Water Resources Planning and Management, *Journal of*
576 *Water Resources Planning and Management*, 132, 129–132,
577 [https://doi.org/10.1061/\(ASCE\)0733-9496\(2006\)132:3\(129\)](https://doi.org/10.1061/(ASCE)0733-9496(2006)132:3(129)), 2006.
- 578 Farley, J. and Costanza, R.: Payments for ecosystem services: From local to global,
579 *Ecological Economics*, 69, 2060–2068, <https://doi.org/10.1016/j.ecolecon.2010.06.010>,
580 2010.
- 581 Gleeson, T., Wang-Erlandsson, L., Zipper, S. C., Porkka, M., Jaramillo, F., Gerten,
582 D., Fetzer, I., Cornell, S. E., Piemontese, L., Gordon, L. J., Rockström, J., Oki, T.,
583 Sivapalan, M., Wada, Y., Brauman, K. A., Flörke, M., Bierkens, M. F. P., Lehner, B.,
584 Keys, P., Kummu, M., Wagener, T., Dadson, S., Troy, T. J., Steffen, W., Falkenmark,
585 M., and Famiglietti, J. S.: The Water Planetary Boundary: Interrogation and Revision,
586 *One Earth*, 2, 223–234, <https://doi.org/10.1016/j.oneear.2020.02.009>, 2020.
- 587 Green, P. A., Vörösmarty, C. J., Harrison, I., Farrell, T., Sáenz, L., and Fekete, B.
588 M.: Freshwater ecosystem services supporting humans: Pivoting from water crisis to

- 589 water solutions, *Global Environmental Change*, 34, 108–118,
590 <https://doi.org/10.1016/j.gloenvcha.2015.06.007>, 2015.
- 591 Hoek van Dijke, A. J., Herold, M., Mallick, K., Benedict, I., Machwitz, M., Schlerf,
592 M., Pranindita, A., Theeuwens, J. J. E., Bastin, J.-F., and Teuling, A. J.: Shifts in regional
593 water availability due to global tree restoration, *Nat. Geosci.*, 15, 363–368,
594 <https://doi.org/10.1038/s41561-022-00935-0>, 2022.
- 595 Hu, H., Tian, G., Wu, Z., and Xia, Q.: Cross-regional ecological compensation
596 under the composite index of water quality and quantity: A case study of the Yellow
597 River Basin, *Environmental Research*, 238, 117152,
598 <https://doi.org/10.1016/j.envres.2023.117152>, 2023.
- 599 Keys, P. W. and Wang-Erlandsson, L.: On the social dynamics of moisture
600 recycling, *Earth System Dynamics*, 9, 829–847, [https://doi.org/10.5194/esd-9-829-](https://doi.org/10.5194/esd-9-829-2018)
601 2018, 2018.
- 602 Keys, P. W., van der Ent, R. J., Gordon, L. J., Hoff, H., Nikoli, R., and Savenije,
603 H. H. G.: Analyzing precipitationsheds to understand the vulnerability of rainfall
604 dependent regions, *Biogeosciences*, 9, 733–746, [https://doi.org/10.5194/bg-9-733-](https://doi.org/10.5194/bg-9-733-2012)
605 2012, 2012.
- 606 Keys, P. W., Barnes, E. A., van der Ent, R. J., and Gordon, L. J.: Variability of
607 moisture recycling using a precipitationshed framework, *Hydrology and Earth System
608 Sciences*, 18, 3937–3950, <https://doi.org/10.5194/hess-18-3937-2014>, 2014.
- 609 Keys, P. W., Wang-Erlandsson, L., Gordon, L. J., Galaz, V., and Ebbesson, J.:
610 Approaching moisture recycling governance, *Global Environmental Change*, 45, 15–
611 23, <https://doi.org/10.1016/j.gloenvcha.2017.04.007>, 2017.
- 612 Keys, P. W., Wang-Erlandsson, L., and Gordon, L. J.: Megacity precipitationsheds
613 reveal tele-connected water security challenges, *PLOS ONE*, 13, e0194311,
614 <https://doi.org/10.1371/journal.pone.0194311>, 2018.
- 615 Keys, P. W., Porkka, M., Wang-Erlandsson, L., Fetzer, I., Gleeson, T., and Gordon,
616 L. J.: Invisible water security: Moisture recycling and water resilience, *Water Security*,
617 8, 100046, <https://doi.org/10.1016/j.wasec.2019.100046>, 2019.
- 618 Lawrence, D. and Vandecar, K.: Effects of tropical deforestation on climate and
619 agriculture, *Nature Clim Change*, 5, 27–36, <https://doi.org/10.1038/nclimate2430>, 2015.
- 620 Li, Y., Piao, S., Li, L. Z. X., Chen, A., Wang, X., Ciais, P., Huang, L., Lian, X.,
621 Peng, S., Zeng, Z., Wang, K., and Zhou, L.: Divergent hydrological response to large-
622 scale afforestation and vegetation greening in China, *Science Advances*, 4, eaar4182,
623 <https://doi.org/10.1126/sciadv.aar4182>, 2018.
- 624 Li, Y., Xu, R., Yang, K., Liu, Y., Wang, S., Zhou, S., Yang, Z., Feng, X., He, C.,
625 Xu, Z., and Zhao, W.: Contribution of Tibetan Plateau ecosystems to local and remote
626 precipitation through moisture recycling, *Global Change Biology*, 29, 702–718,
627 <https://doi.org/10.1111/gcb.16495>, 2023.
- 628 McDermid, S., Nocco, M., Lawston-Parker, P., Keune, J., Pokhrel, Y., Jain, M.,
629 Jägermeyr, J., Brocca, L., Massari, C., Jones, A. D., Vahmani, P., Thiery, W., Yao, Y.,
630 Bell, A., Chen, L., Dorigo, W., Hanasaki, N., Jasechko, S., Lo, M.-H., Mahmood, R.,
631 Mishra, V., Mueller, N. D., Niyogi, D., Rabin, S. S., Sloat, L., Wada, Y., Zappa, L., Chen,
632 F., Cook, B. I., Kim, H., Lombardozzi, D., Polcher, J., Ryu, D., Santanello, J., Satoh,
633 Y., Seneviratne, S., Singh, D., and Yokohata, T.: Irrigation in the Earth system, *Nat Rev
634 Earth Environ*, <https://doi.org/10.1038/s43017-023-00438-5>, 2023.

- 635 Munia, H., Guillaume, J. H. A., Mirumachi, N., Porkka, M., Wada, Y., and Kummu,
636 M.: Water stress in global transboundary river basins: significance of upstream water
637 use on downstream stress, *Environ. Res. Lett.*, 11, 014002,
638 <https://doi.org/10.1088/1748-9326/11/1/014002>, 2016.
- 639 O'Connor, J. C., Dekker, S. C., Staal, A., Tuinenburg, O. A., Rebel, K. T., and
640 Santos, M. J.: Forests buffer against variations in precipitation, *Global Change Biology*,
641 27, 4686–4696, <https://doi.org/10.1111/gcb.15763>, 2021.
- 642 Pissarra, T. C. T., Sanches Fernandes, L. F., and Pacheco, F. A. L.: Production of
643 clean water in agriculture headwater catchments: A model based on the payment for
644 environmental services, *Science of The Total Environment*, 785, 147331,
645 <https://doi.org/10.1016/j.scitotenv.2021.147331>, 2021.
- 646 Pranindita, A., Wang-Erlandsson, L., Fetzer, I., and Teuling, A. J.: Moisture
647 recycling and the potential role of forests as moisture source during European
648 heatwaves, *Clim Dyn*, 58, 609–624, <https://doi.org/10.1007/s00382-021-05921-7>, 2022.
- 649 Qin, Y.: Global competing water uses for food and energy, *Environ. Res. Lett.*, 16,
650 064091, <https://doi.org/10.1088/1748-9326/ac06fa>, 2021.
- 651 Rockström, J., Mazzucato, M., Andersen, L. S., Fahrländer, S. F., and Gerten, D.:
652 Why we need a new economics of water as a common good, *Nature*, 615, 794–797,
653 <https://doi.org/10.1038/d41586-023-00800-z>, 2023.
- 654 Schyns, J. F., Hoekstra, A. Y., Booij, M. J., Hogeboom, R. J., and Mekonnen, M.
655 M.: Limits to the world's green water resources for food, feed, fiber, timber, and
656 bioenergy, *Proceedings of the National Academy of Sciences*, 116, 4893–4898,
657 <https://doi.org/10.1073/pnas.1817380116>, 2019.
- 658 Shao, R., Zhang, B., Su, T., Long, B., Cheng, L., Xue, Y., and Yang, W.: Estimating
659 the Increase in Regional Evaporative Water Consumption as a Result of Vegetation
660 Restoration Over the Loess Plateau, China, *Journal of Geophysical Research:*
661 *Atmospheres*, 124, 11783–11802, <https://doi.org/10.1029/2019JD031295>, 2019.
- 662 Sheng, J. and Webber, M.: Incentive coordination for transboundary water
663 pollution control: The case of the middle route of China's South-North water Transfer
664 Project, *Journal of Hydrology*, 598, 125705,
665 <https://doi.org/10.1016/j.jhydrol.2020.125705>, 2021.
- 666 Staal, A., Koren, G., Tejada, G., and Gatti, L. V.: Moisture origins of the Amazon
667 carbon source region, *Environ. Res. Lett.*, 18, 044027, <https://doi.org/10.1088/1748-9326/acc676>, 2023.
- 669 Su, Y., Li, X., Feng, M., Nian, Y., Huang, L., Xie, T., Zhang, K., Chen, F., Huang,
670 W., Chen, J., and Chen, F.: High agricultural water consumption led to the continued
671 shrinkage of the Aral Sea during 1992–2015, *Science of The Total Environment*, 777,
672 145993, <https://doi.org/10.1016/j.scitotenv.2021.145993>, 2021.
- 673 Sun, G., Zhou, G., Zhang, Z., Wei, X., McNulty, S. G., and Vose, J. M.: Potential
674 water yield reduction due to forestation across China, *Journal of Hydrology*, 328, 548–
675 558, <https://doi.org/10.1016/j.jhydrol.2005.12.013>, 2006.
- 676 Sun, Y., Clemens, S. C., Morrill, C., Lin, X., Wang, X., and An, Z.: Influence of
677 Atlantic meridional overturning circulation on the East Asian winter monsoon, *Nature*
678 *Geosci*, 5, 46–49, <https://doi.org/10.1038/ngeo1326>, 2012.
- 679 Theeuwens, J. J. E., Staal, A., Tuinenburg, O. A., Hamelers, B. V. M., and Dekker,

- 680 S. C.: Local moisture recycling across the globe, *Hydrology and Earth System Sciences*,
681 27, 1457–1476, <https://doi.org/10.5194/hess-27-1457-2023>, 2023.
- 682 Tian, B. and Fan, K.: Factors favorable to frequent extreme precipitation in the
683 upper Yangtze River Valley, *Meteorol Atmos Phys*, 121, 189–197,
684 <https://doi.org/10.1007/s00703-013-0261-9>, 2013.
- 685 Tuinenburg, O. A. and Staal, A.: Tracking the global flows of atmospheric
686 moisture and associated uncertainties, *Hydrology and Earth System Sciences*, 24,
687 2419–2435, <https://doi.org/10.5194/hess-24-2419-2020>, 2020.
- 688 Tuinenburg, O. A., Theeuwes, J. J. E., and Staal, A.: High-resolution global
689 atmospheric moisture connections from evaporation to precipitation, *Earth System
690 Science Data*, 12, 3177–3188, <https://doi.org/10.5194/essd-12-3177-2020>, 2020.
- 691 Varis, O. and Vakkilainen, P.: China’s 8 challenges to water resources management
692 in the first quarter of the 21st Century, *Geomorphology*, 41, 93–104,
693 [https://doi.org/10.1016/S0169-555X\(01\)00107-6](https://doi.org/10.1016/S0169-555X(01)00107-6), 2001.
- 694 Veldkamp, T. I. E., Wada, Y., Aerts, J. C. J. H., Döll, P., Gosling, S. N., Liu, J.,
695 Masaki, Y., Oki, T., Ostberg, S., Pokhrel, Y., Satoh, Y., Kim, H., and Ward, P. J.: Water
696 scarcity hotspots travel downstream due to human interventions in the 20th and 21st
697 century, *Nat Commun*, 8, 15697, <https://doi.org/10.1038/ncomms15697>, 2017.
- 698 Viviroli, D., Kumm, M., Meybeck, M., Kallio, M., and Wada, Y.: Increasing
699 dependence of lowland populations on mountain water resources, *Nat Sustain*, 3, 917–
700 928, <https://doi.org/10.1038/s41893-020-0559-9>, 2020.
- 701 Wang, S., Fu, B., Liang, W., Liu, Y., and Wang, Y.: Driving forces of changes in
702 the water and sediment relationship in the Yellow River, *Science of The Total
703 Environment*, 576, 453–461, <https://doi.org/10.1016/j.scitotenv.2016.10.124>, 2017.
- 704 Wang, X., Zhang, Z., Zhang, B., Tian, L., Tian, J., Arnault, J., Kunstmann, H., and
705 He, C.: Quantifying the Impact of Land Use and Land Cover Change on Moisture
706 Recycling With Convection-Permitting WRF-Tagging Modeling in the Agro-Pastoral
707 Ecotone of Northern China, *Journal of Geophysical Research: Atmospheres*, 128,
708 e2022JD038421, <https://doi.org/10.1029/2022JD038421>, 2023a.
- 709 Wang, Y., Liu, X., Zhang, D., and Bai, P.: Tracking Moisture Sources of
710 Precipitation Over China, *Journal of Geophysical Research: Atmospheres*, 128,
711 e2023JD039106, <https://doi.org/10.1029/2023JD039106>, 2023b.
- 712 Wang-Erlandsson, L., Fetzer, I., Keys, P. W., van der Ent, R. J., Savenije, H. H. G.,
713 and Gordon, L. J.: Remote land use impacts on river flows through atmospheric
714 teleconnections, *Hydrology and Earth System Sciences*, 22, 4311–4328,
715 <https://doi.org/10.5194/hess-22-4311-2018>, 2018.
- 716 Wang-Erlandsson, L., Tobian, A., van der Ent, R. J., Fetzer, I., te Wierik, S., Porkka,
717 M., Staal, A., Jaramillo, F., Dahmann, H., Singh, C., Greve, P., Gerten, D., Keys, P. W.,
718 Gleeson, T., Cornell, S. E., Steffen, W., Bai, X., and Rockström, J.: A planetary
719 boundary for green water, *Nat Rev Earth Environ*, 3, 380–392,
720 <https://doi.org/10.1038/s43017-022-00287-8>, 2022.
- 721 Wei, F., Wang, S., Fu, B., Li, Y., Huang, Y., Zhang, W., and Fensholt, R.:
722 Quantifying the precipitation supply of China’s drylands through moisture recycling,
723 *Agricultural and Forest Meteorology*, 352, 110034,
724 <https://doi.org/10.1016/j.agrformet.2024.110034>, 2024.

- 725 Weng, W., Luedeke, M. K. B., Zemp, D. C., Lakes, T., and Kropp, J. P.: Aerial and
726 surface rivers: downwind impacts on water availability from land use changes in
727 Amazonia, *Hydrology and Earth System Sciences*, 22, 911–927,
728 <https://doi.org/10.5194/hess-22-911-2018>, 2018.
- 729 te Wierik, S. A., Cammeraat, E. L. H., Gupta, J., and Artzy-Randrup, Y. A.:
730 Reviewing the Impact of Land Use and Land-Use Change on Moisture Recycling and
731 Precipitation Patterns, *Water Resources Research*, 57, e2020WR029234,
732 <https://doi.org/10.1029/2020WR029234>, 2021.
- 733 Wu, B. and Wang, J.: Winter Arctic Oscillation, Siberian High and East Asian
734 Winter Monsoon, *Geophysical Research Letters*, 29, 3-1-3-4,
735 <https://doi.org/10.1029/2002GL015373>, 2002.
- 736 Xie, D., Zhang, Y., Zhang, M., Tian, Y., Cao, Y., Mei, Y., Liu, S., and Zhong, D.:
737 Hydrological impacts of vegetation cover change in China through terrestrial moisture
738 recycling, *Science of The Total Environment*, 915, 170015,
739 <https://doi.org/10.1016/j.scitotenv.2024.170015>, 2024.
- 740 Ya-Feng, Z., Min, D., Ya-Jing, L., and Yao, R.: Evolution characteristics and policy
741 implications of new urbanization in provincial capital cities in Western China, *PLoS*
742 *ONE*, 15, e0233555, <https://doi.org/10.1371/journal.pone.0233555>, 2020.
- 743 Yang, Z., Qian, Y., Liu, Y., Berg, L. K., Hu, H., Dominguez, F., Yang, B., Feng, Z.,
744 Gustafson Jr, W. I., Huang, M., and Tang, Q.: Irrigation Impact on Water and Energy
745 Cycle During Dry Years Over the United States Using Convection-Permitting WRF and
746 a Dynamical Recycling Model, *Journal of Geophysical Research: Atmospheres*, 124,
747 11220–11241, <https://doi.org/10.1029/2019JD030524>, 2019.
- 748 Zemp, D. C., Schleussner, C.-F., Barbosa, H. M. J., van der Ent, R. J., Donges, J.
749 F., Heinke, J., Sampaio, G., and Rammig, A.: On the importance of cascading moisture
750 recycling in South America, *Atmospheric Chemistry and Physics*, 14, 13337–13359,
751 <https://doi.org/10.5194/acp-14-13337-2014>, 2014.
- 752 Zhang, B., Tian, L., Zhao, X., and Wu, P.: Feedbacks between vegetation
753 restoration and local precipitation over the Loess Plateau in China, *Sci. China Earth*
754 *Sci.*, 64, 920–931, <https://doi.org/10.1007/s11430-020-9751-8>, 2021.
- 755 Zhang, B., Gao, H., and Wei, J.: Identifying potential hotspots for atmospheric
756 water resource management and source-sink analysis, *CSB*, 68, 2678–2689,
757 <https://doi.org/10.1360/TB-2022-1275>, 2023.
- 758 Zhang, C., Zhang, X., Tang, Q., Chen, D., Huang, J., Wu, S., and Liu, Y.:
759 Quantifying precipitation moisture contributed by different atmospheric circulations
760 across the Tibetan Plateau, *Journal of Hydrology*, 628, 130517,
761 <https://doi.org/10.1016/j.jhydrol.2023.130517>, 2024.
- 762 Zhao, Y. and Zhou, T.: Interannual Variability of Precipitation Recycle Ratio Over
763 the Tibetan Plateau, *Journal of Geophysical Research: Atmospheres*, 126,
764 e2020JD033733, <https://doi.org/10.1029/2020JD033733>, 2021.
- 765 Zhou, G., Wei, X., Chen, X., Zhou, P., Liu, X., Xiao, Y., Sun, G., Scott, D. F., Zhou,
766 S., Han, L., and Su, Y.: Global pattern for the effect of climate and land cover on water
767 yield, *Nat Commun*, 6, 5918, <https://doi.org/10.1038/ncomms6918>, 2015a.
- 768 Zhou, Y., Huang, H. Q., Nanson, G. C., Huang, C., and Liu, G.: Progradation of
769 the Yellow (Huanghe) River delta in response to the implementation of a basin-scale
770 water regulation program, *Geomorphology*, 243, 65–74,

773 **Appendix A**

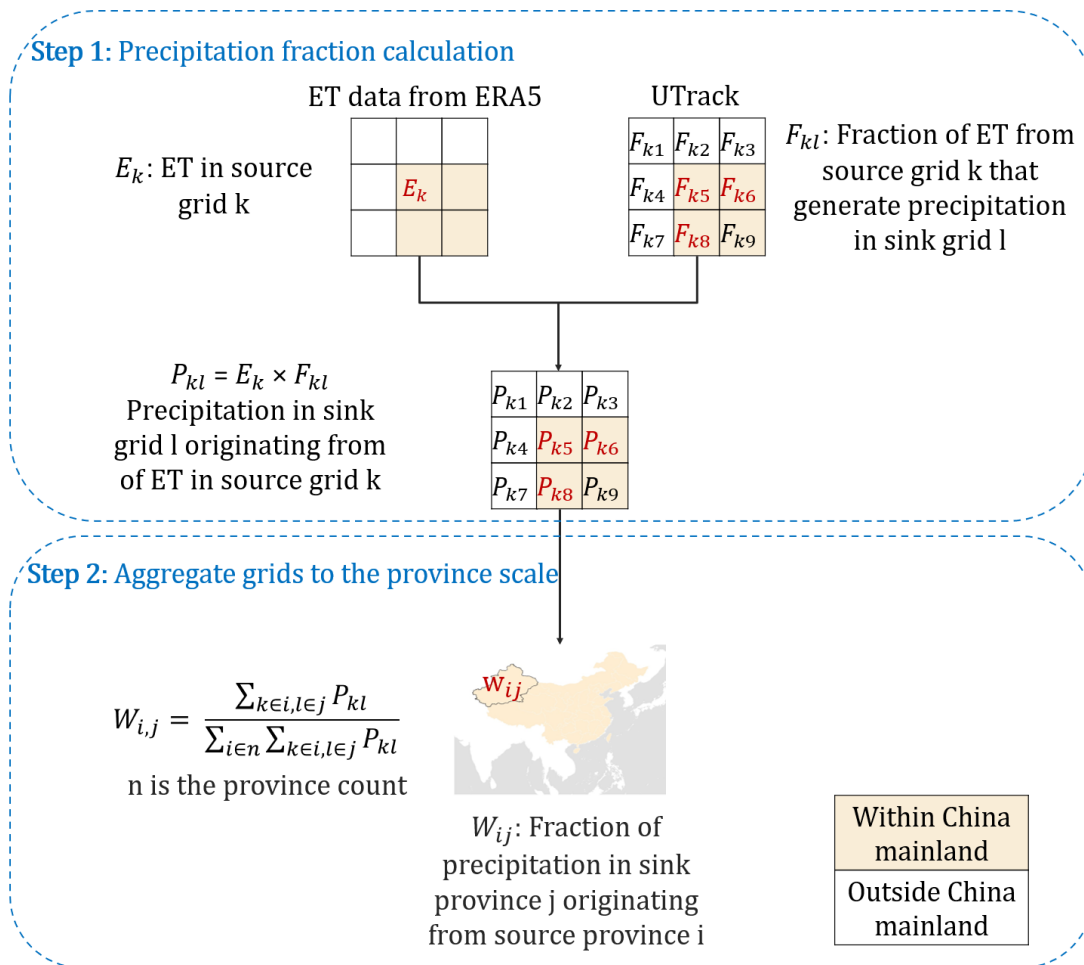
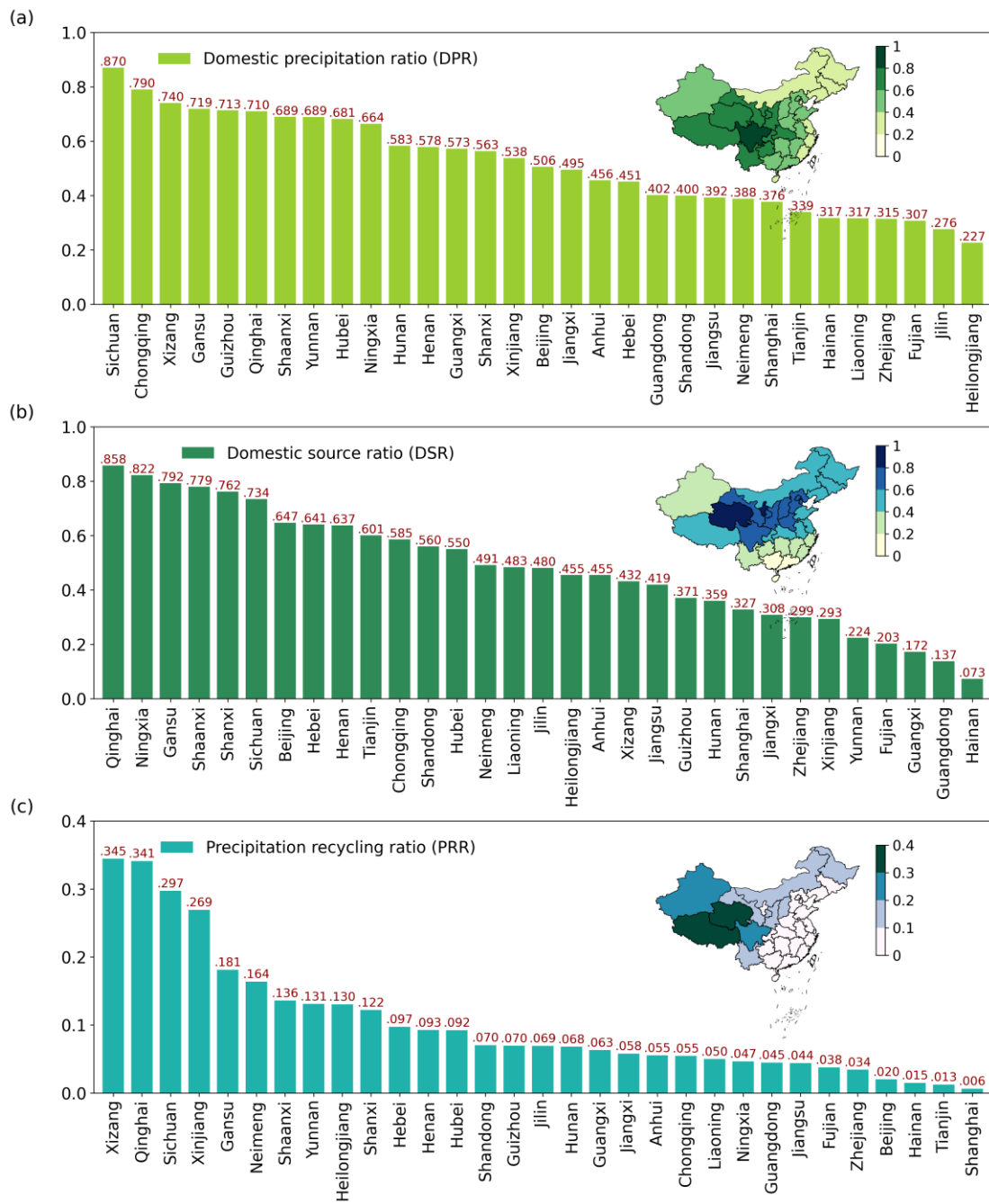
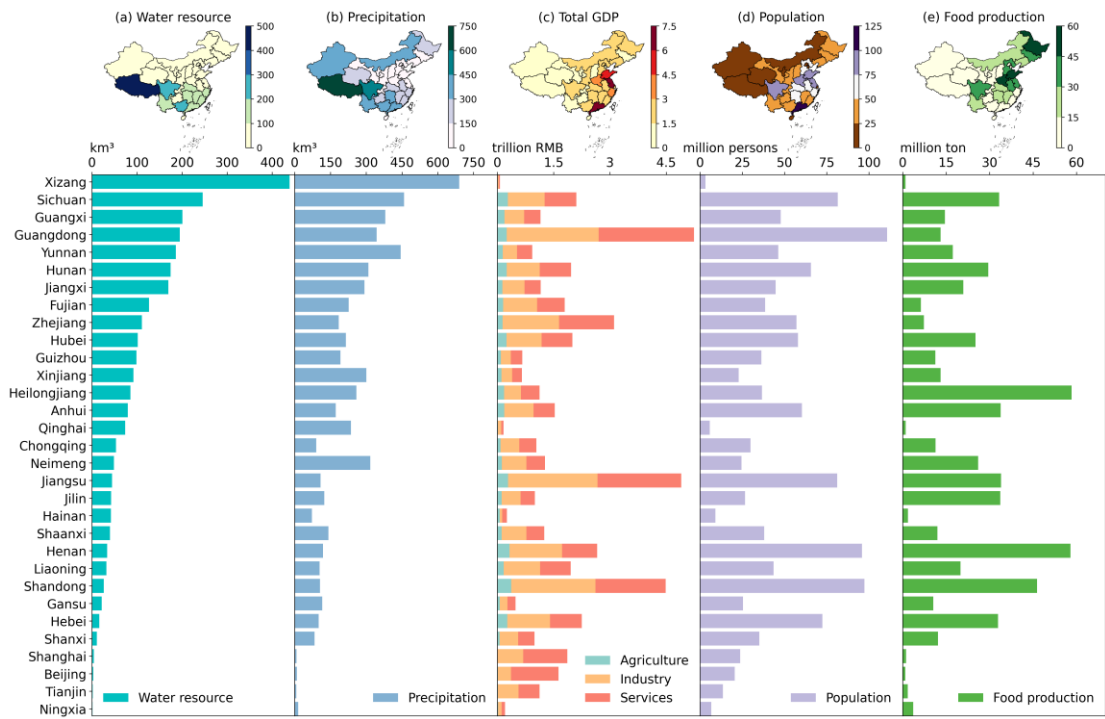


Figure A1. Workflow of estimating green water flow. Step 1: calculate the precipitation in sink grids originating from ET in source grids. Step 2: calculate the fraction of precipitation in sink provinces originating from source provinces.



779
780
781
782

Figure A2. (a) Domestic precipitation ratio (DPR), (b) domestic source ratio (DSR) and (c) precipitation recycling ratio (PRR) in each province.



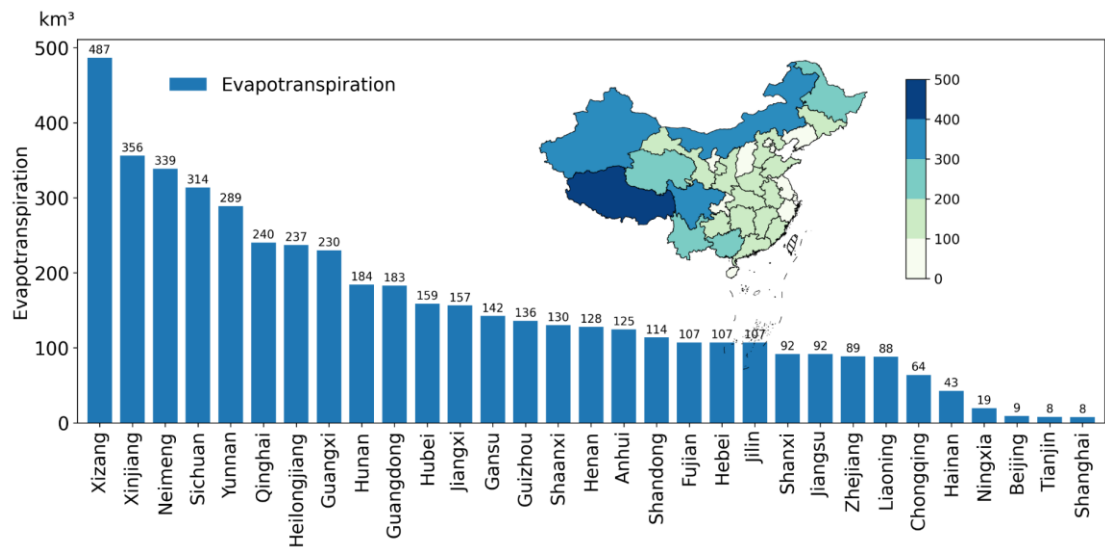
783

784

Figure A3. Water resource (a), precipitation (b), GDP (c), population (d) and food production (e) in each province.

785

786

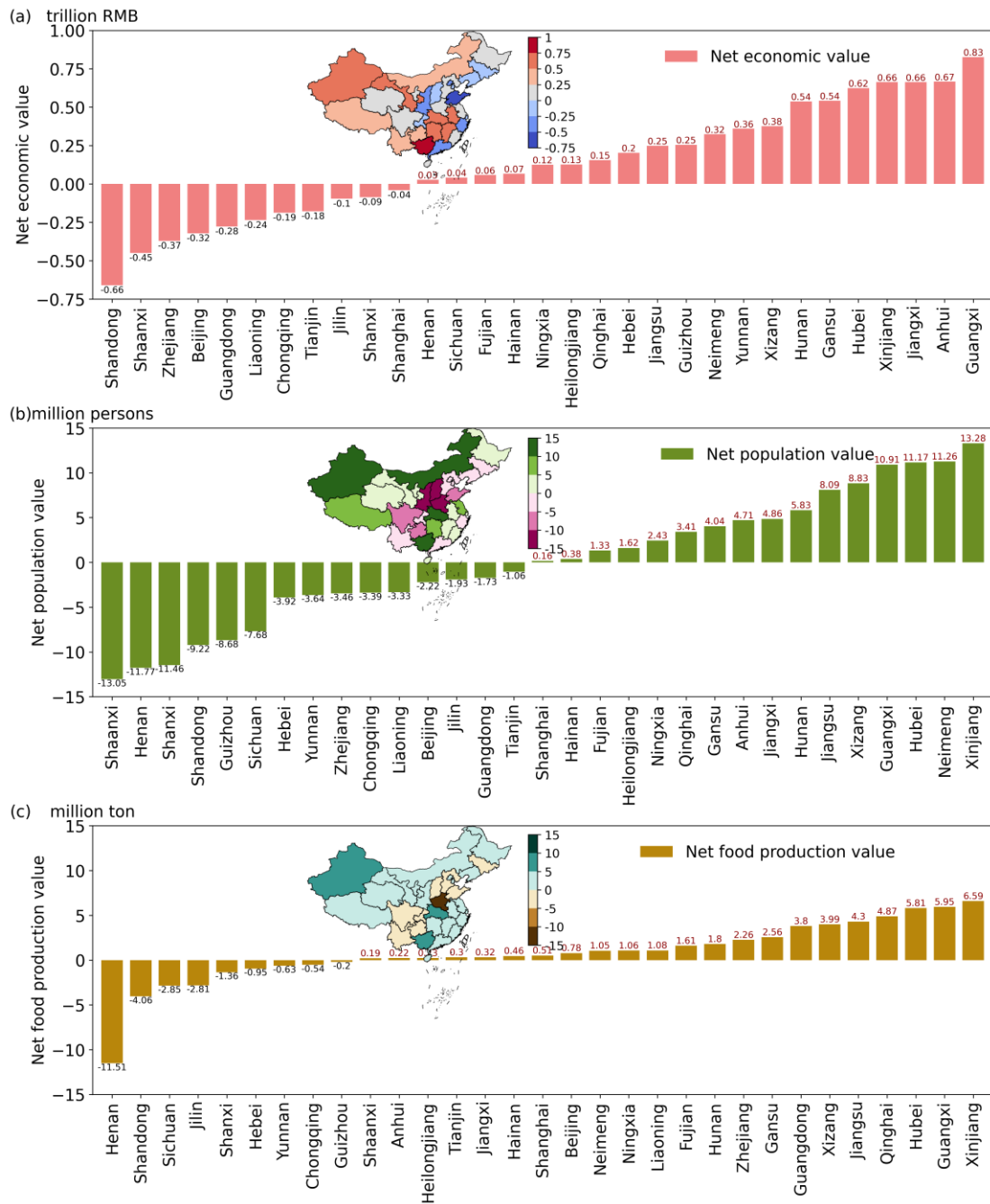


787

788

Figure A4. Mean evapotranspiration of 2008 to 2017 in each province.

789



790

791

Figure A5. Net economic output (a), population (b), food production (c) value of green water flow

792

in each province. Negative values represent these socio-economic values of water resource formed

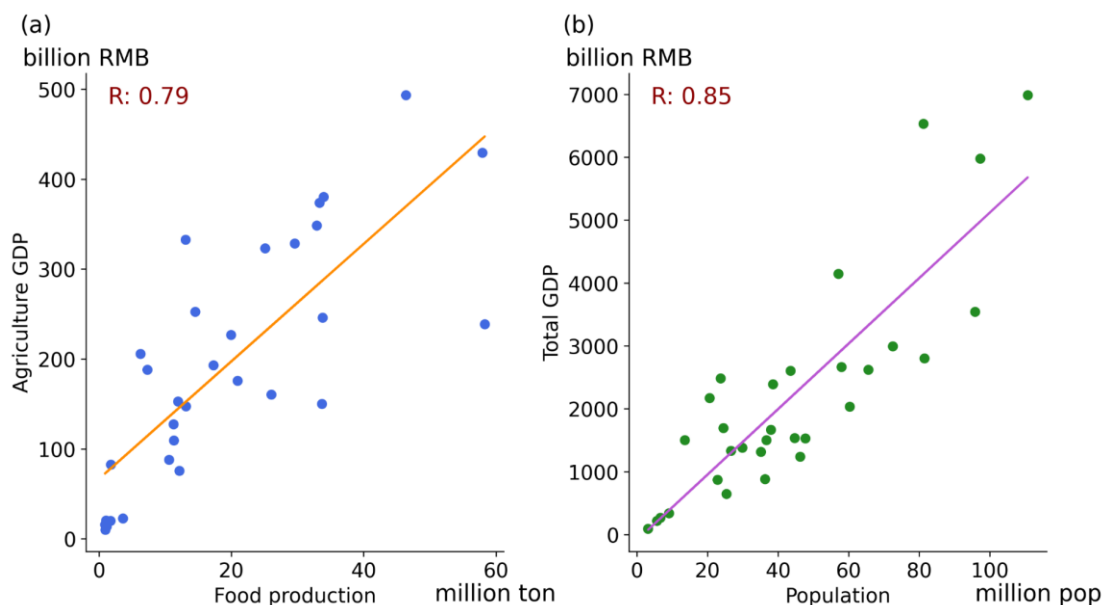
793

by green water increase by flowing from source to sink provinces. Positive values represent these

794

socio-economic values of water resource formed by green water decrease by flowing.

795



796

797 **Figure A6.** Spatial pearson correlation coefficient between agricultural GDP and food production
 798 (a), population and total GDP (b) across provinces in China.

799

800 **Table A1.** Precipitation, water resources, and the contribution from green water in provinces of
 801 China.

Province	Local precipitation (km ³)	Precipitation formed by green water (km ³)	Percentage of precipitation contribution to local precipitation (%)	Local water resource (km ³)	Water resource formed by green water (km ³)	Percentage of water resource contribution to local water resource (%)
Beijing	9.47	4.53	48	2.82	1.14	40
Tianjin	7.12	2.66	37	1.62	0.70	43
Hebei	100.50	48.35	48	15.98	12.26	77
Shanxi	82.88	51.69	62	10.91	12.38	113
Neimeng	317.11	131.57	41	48.79	31.80	65
Liaoning	104.53	27.80	27	31.92	8.40	26
Jilin	124.15	29.55	24	42.21	8.98	21
Heilongjiang	258.88	53.75	21	85.40	15.44	18
Shanghai	8.02	2.83	35	4.04	1.19	29
Jiangsu	108.09	35.93	33	44.27	13.43	30
Zhejiang	184.72	27.98	15	110.66	13.46	12
Anhui	172.36	56.84	33	79.67	23.19	29
Fujian	226.74	32.96	15	126.39	17.33	14
Jiangxi	292.56	77.52	26	169.44	39.25	23
Shandong	105.99	45.49	43	25.99	13.56	52
Henan	118.83	73.87	62	33.73	24.08	71
Hubei	214.46	108.13	50	101.66	45.27	45

Hunan	308.87	107.25	35	174.33	52.28	30
Guangdong	344.05	73.31	21	194.77	38.54	20
Guangxi	379.82	131.63	35	200.76	66.32	33
Hainan	72.47	13.50	19	41.86	7.13	17
Chongqing	90.61	50.45	56	53.23	21.87	41
Sichuan	458.97	272.93	59	245.86	124.43	51
Guizhou	191.84	97.05	51	98.49	46.54	47
Yunnan	444.68	199.06	45	185.99	96.34	52
Xizang	689.68	360.21	52	438.59	200.33	46
Shaanxi	141.21	89.70	64	39.82	26.14	66
Gansu	115.45	102.36	89	21.60	30.31	140
Qinghai	236.12	170.62	72	73.50	63.57	86
Ningxia	14.95	12.94	87	0.98	3.34	342
Xinjiang	300.10	191.37	64	91.95	64.92	71
Total	6225.19	2683.84	43	2.82	1.14	40

802

803 **Table A2.** The embodied socio-economic values of green water flow from source
804 provinces for water resources, GDP by industry, population, and food production.

805 Socio-economic indicators are the average value of 2008-2017.

Province	Total GDP (Trillion CNY)	Agriculture GDP (Trillion CNY)	Industry GDP (Trillion CNY)	Service GDP (Trillion CNY)	Population (Million persons)	Food production (Million ton)
Beijing	0.13	0.01	0.05	0.07	2.05	0.97
Tianjin	0.09	0.01	0.04	0.04	1.33	0.61
Hebei	1.27	0.09	0.56	0.62	22	10.82
Shanxi	1.18	0.09	0.54	0.55	22.36	10.35
Neimeng	1.67	0.15	0.77	0.75	30.77	21.78
Liaoning	0.40	0.04	0.19	0.17	7.23	5.92
Jilin	0.27	0.03	0.12	0.11	5.34	6.37
Heilongjiang	0.39	0.05	0.17	0.17	8.04	10.45
Shanghai	0.09	0.01	0.04	0.04	1.41	0.57
Jiangsu	1.06	0.08	0.51	0.47	18.13	8.5
Zhejiang	0.69	0.04	0.32	0.32	11.08	4.11
Anhui	1.37	0.11	0.66	0.59	25.42	11.85
Fujian	0.56	0.04	0.27	0.26	9.46	2.93
Jiangxi	1.33	0.10	0.64	0.59	24.34	9.43
Shandong	1.37	0.11	0.65	0.62	23.85	11.72
Henan	1.75	0.15	0.85	0.75	34.94	16.74
Hubei	1.98	0.18	0.96	0.84	40.57	18.56
Hunan	1.63	0.15	0.78	0.70	33.2	14.13

Guangdong	1.10	0.08	0.52	0.49	20.09	6.38
Guangxi	1.54	0.14	0.73	0.67	33.06	12.7
Hainan	0.18	0.01	0.08	0.08	3.42	1.05
Chongqing	0.66	0.06	0.32	0.28	14.92	6.4
Sichuan	2.31	0.25	1.10	0.96	58.39	24.16
Guizhou	1.08	0.11	0.51	0.46	25.05	10.25
Yunnan	1.48	0.16	0.69	0.63	38.21	14.98
Xizang	0.56	0.07	0.26	0.23	15.32	5.97
Shaanxi	1.48	0.13	0.71	0.64	30.87	14
Gansu	1.05	0.10	0.50	0.46	24.22	10.96
Qinghai	0.72	0.07	0.34	0.31	18.3	7.56
Ningxia	0.18	0.02	0.09	0.08	3.88	1.85
Xinjiang	1.00	0.11	0.46	0.43	22.03	11.6
Total (percentage of total contribution to local socio-economic value)	30.56 (45%)	2.74 (46%)	14.43 (45%)	13.39 (44%)	629.28 (46%)	293.67 (50%)

806